Supplementary Information

Synthesis, Characterization, and Device Application of Antimony-Substituted Violet Phosphorus – A Layered Material

Franziska Baumer[a#], Yuqiang Ma[b#], Chenfei Shen[b#], Anyi Zhang[b], Liang Chen[b], Yihang Liu[b], Daniela Pfister[a], Tom Nilges[a*] and Chongwu Zhou[b*]

[#]Authors contributed equally to this work

***Corresponding author: Tom Nilges,** Department für Chemie, Technische Universität München, Lichtenbergstrasse 4, 85747 Garching b. München, Germany, e-mail: tom.nilges@lrz.tum.de

***Corresponding author: Chongwu Zhou,** Department of electrical Engineering, University of Southern California, 3710 McClintock Ave, Los Angeles, CA 90089-0271, USA, e-mail: chongwuz@usc.edu

[a]**Franziska Baumer, Daniela Pfister:** Department für Chemie, Technische Universität München, Lichtenbergstrasse 4, 85747 Garching b. München, Germany

[b]**Yuqiang Ma, Chenfei Shen, Anyi Zhang, Liang Chen, Yihang Liu:** Department of Electrical Engineering, University of Southern California, 3710 McClintock Ave, Los Angeles, CA 90089-0271, USA

Supporting Information. SEM, XRD, optical images, I-V measurements, AFM measurements, and tables of crystal structure parameters of antimony-substituted violet phosphorus.

Table S1. Comparison of properties among 4 phosphorus-related materials. The parameters of *Hittorf's* phosphorus, black arsenic-phosphorus and black phosphorus are reported by literatures.[1-4]

Material	Bandgap	Experimental Mobility	Stability in air
antimony-substituted *Hittorf's* phosphorus	1.67 eV	43.08 $cm^2/V{\cdot}s$	Reasonable stability
Hittorf's phosphorus	2.5 eV	Not reported yet	Stable
black arsenic–phosphorus	0.15 eV	110 $cm^2/V{\cdot}s$	Prone to oxidation
black phosphorus	0.3 eV (bulk) 2.2 eV (monolayer)	>400 $cm^2/V{\cdot}s$	Prone to oxidation

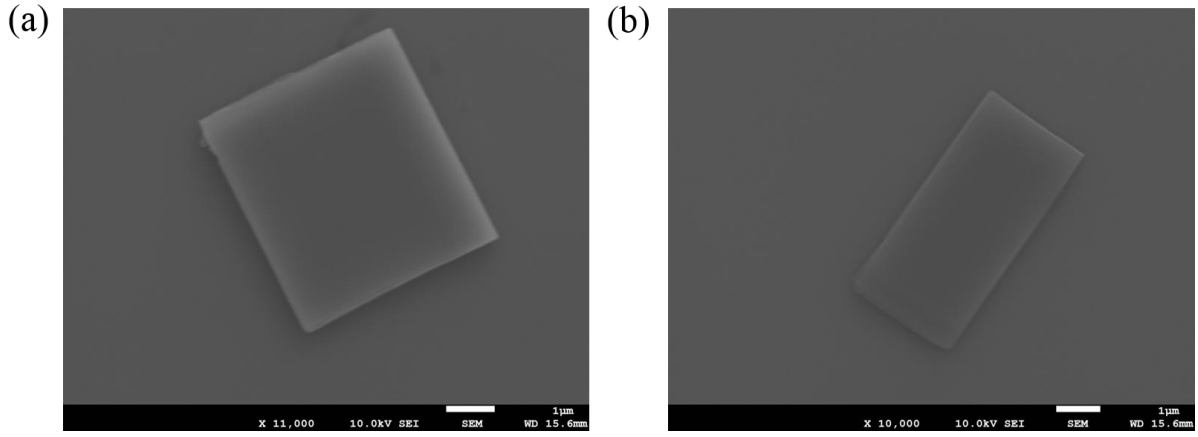

Figure S1. SEM images of two typical PSb thin flakes. The sharp edges can be observed from these samples.

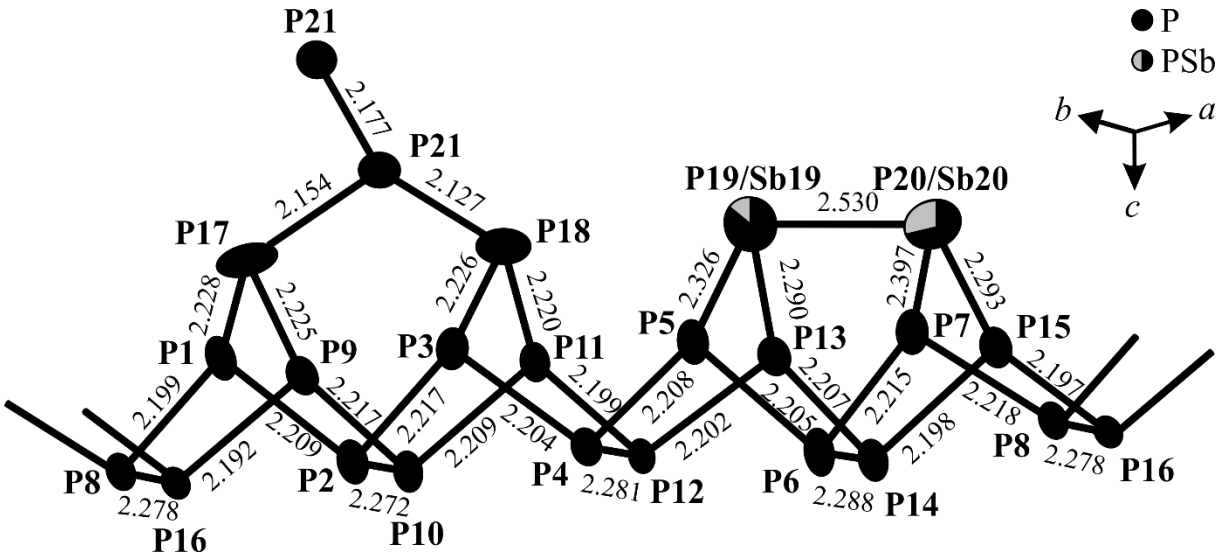

Figure S2. [P9]P2[P8]P2[substructure of $P_{20.56(1)}Sb_{0.44(1)}$. Bond lengths are given in [Å]. Ellipsoids show 80% probability for atomic displacement.

Powder X-ray powder diffraction (PXRD) measurements

Single crystals of $P_{20.56(1)}Sb_{0.44(1)}$ were subject to X-ray phase analysis. Due to tendency of the $P_{20.56(1)}Sb_{0.44(1)}$ crystals to cleave upon grinding, selected crystals of approximately 0.5 mm in length and 100 μm in diameter were measured without any pretreatment directly on a flat-bed sample holder. Due to the restrictions of measurement conditions and the low amount of scattering material in the X-ray beam, a large background was observed after a 48 h measurement. No reflections of any other crystalline phase that the title compound was observed.

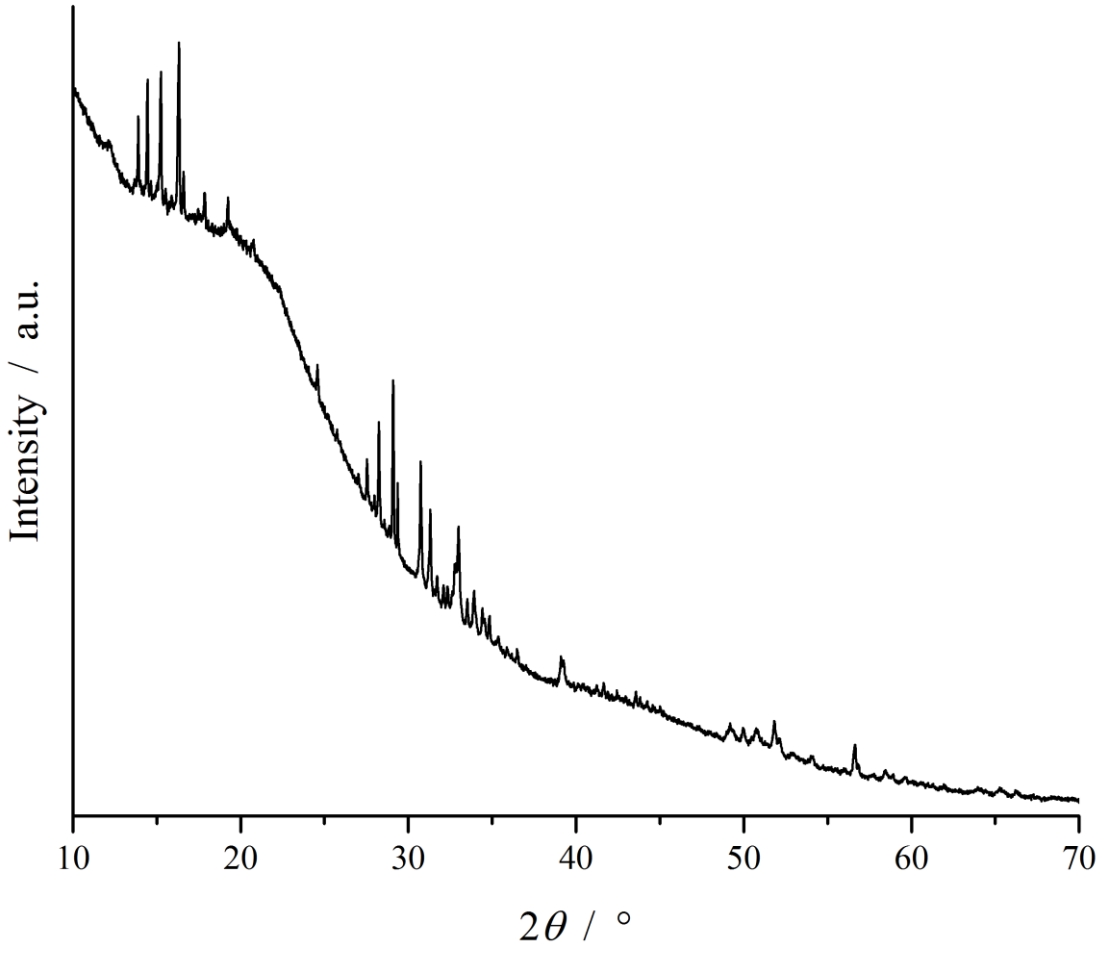

Figure S3. PXRD pattern of Sb-substituted *Hittorf's* phosphorus $P_{20.56(1)}Sb_{0.44(1)}$.

Differential scanning calorimetry (DSC) measurements

Phase pure PSb was used for thermal analysis. The sample was transferred under argon atmosphere to an aluminium crucible and investigated with a NETZSCH DSC 200 F3 Maja using cooling and heating rate of 10 K/min. No thermal effect was found in the temperature range of 113-673 K substantiating that Sb-substituted violet phosphorus is stable up to this temperature in argon atmosphere.

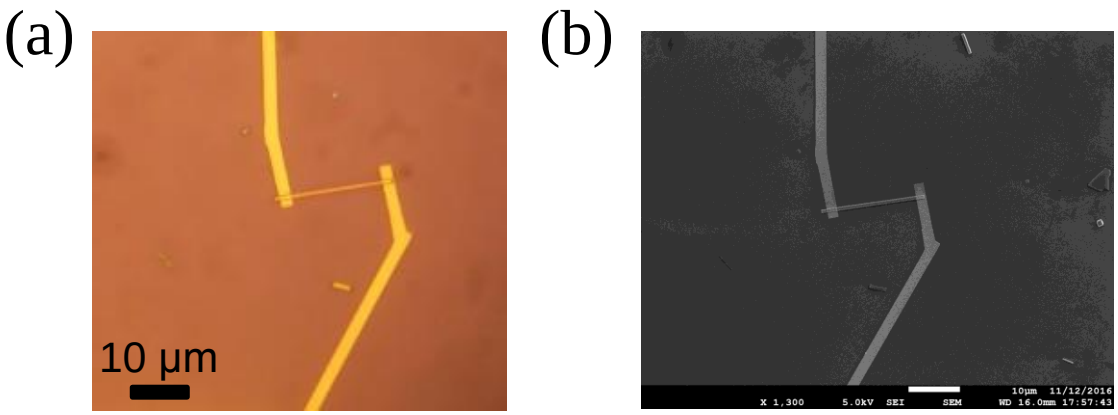

Figure S4. The (a) optical image and (b) SEM image of the same device shown in Figure 6b. For the yellow electrodes, 3 nm Ti and 30 nm Au double-layer structure is used.

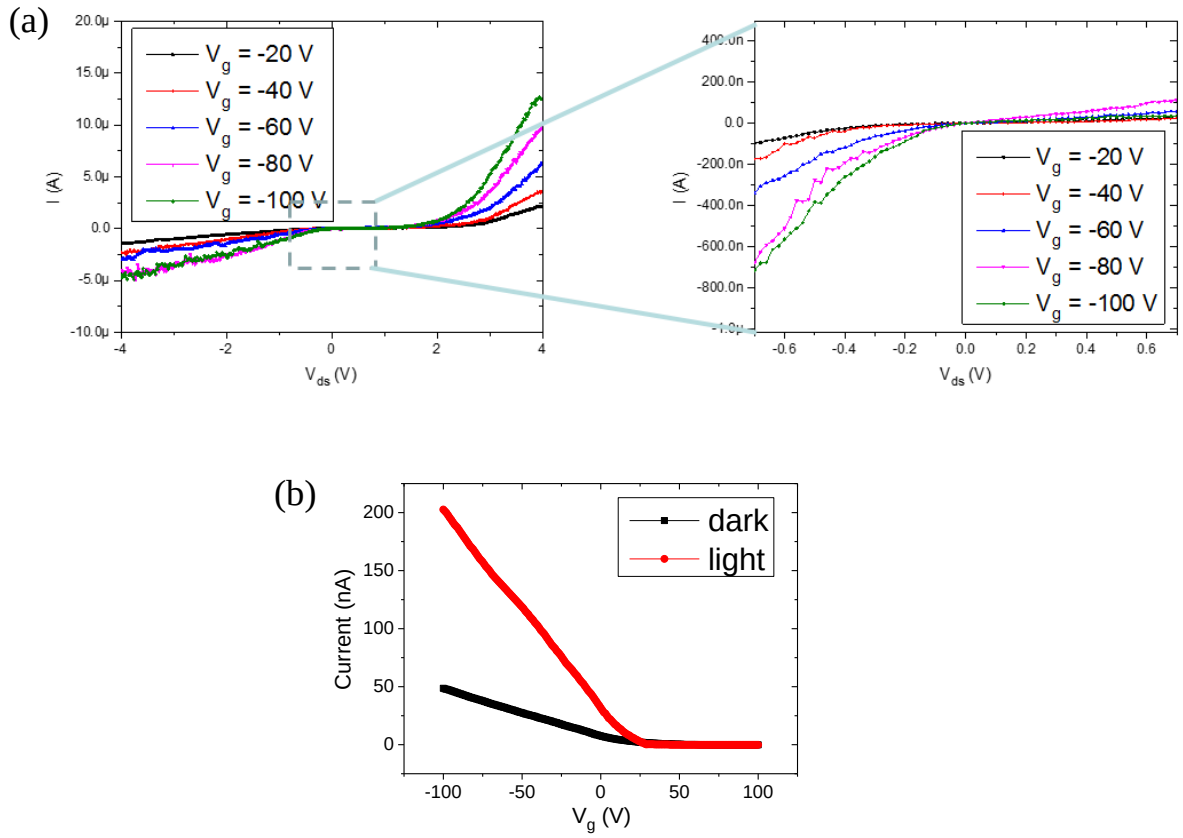

Figure S5. Electrical measurements of the PSb devices. (a) The I_{ds}-V_{ds} family curves for the same device shown in Figure S4. (b) Measurements of dark current and light current of a PSb device.

Figure S6. An optical image of $P_{20.56(1)}Sb_{0.44(1)}$ located inside an ampoule after synthesis. On the left-hand side the bulky residue is a lead regulus, while on the right hand side are bundles of fine needle-shaped $P_{20.56(1)}Sb_{0.44(1)}$.

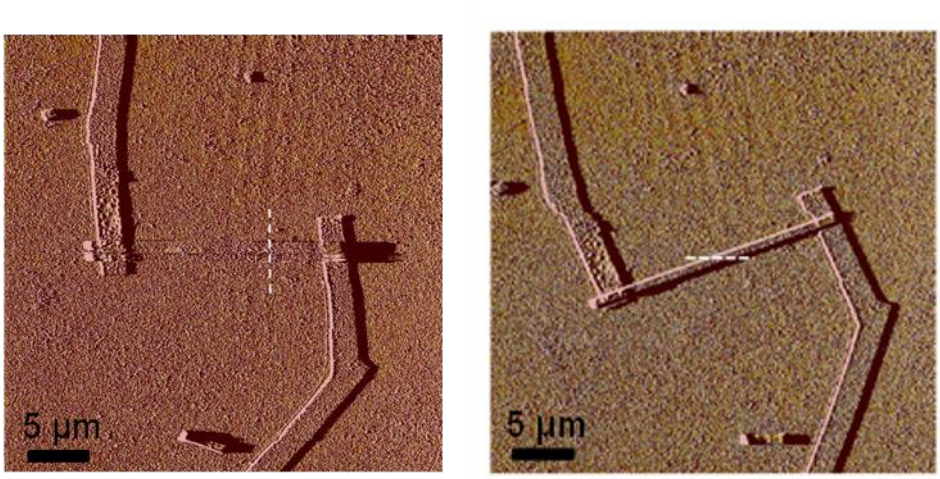

Figure S7. AFM measurements of the same PSb flake with a time separation of 1 month. The left one is the earlier scan. No degradation is detected.

Table S2: Atomic coordinates, SOF and U_{eq} [Å^2] of $P_{20.56(1)}Sb_{0.44(1)}$, space group $P2/c$.

Atom	SOF	*x*	*y*	*z*	U_{eq}
P1	1	0.44661(17)	0.05554(16)	0.32176(7)	0.0239(5)
P2	1	0.67572(16)	0.02820(16)	0.61404(8)	0.0255(5)
P3	1	0.20000(17)	0.19518(16)	0.82045(7)	0.0246(5)
P4	1	0.07569(16)	0.72342(16)	0.38401(7)	0.0210(5)
P5	1	0.06292(16)	0.55304(16)	0.17405(7)	0.0250(5)
P6	1	0.18165(16)	0.48219(16)	0.10680(8)	0.0255(5)
P7	1	0.29926(17)	0.31999(17)	0.17606(7)	0.0253(5)
P8	1	0.42458(16)	0.22198(16)	0.11527(7)	0.0220(5)
P9	1	0.29139(15)	0.13552(16)	0.57208(7)	0.0217(5)
P10	1	0.50022(16)	0.15570(17)	0.54251(7)	0.0229(5)
P11	1	0.54036(16)	0.61422(16)	0.07134(7)	0.0225(5)
P12	1	0.25029(15)	0.59550(16)	0.45651(7)	0.0185(4)
P13	1	0.19956(15)	0.36459(16)	0.43323(7)	0.0230(5)
P14	1	0.00624(15)	0.35048(17)	0.03556(7)	0.0229(5)
P15	1	0.03609(15)	0.12363(16)	0.06794(7)	0.0223(5)
P16	1	0.24875(15)	0.09335(16)	0.04381(7)	0.0193(4)
P17	1	0.3662(2)	0.1013(2)	0.67342(8)	0.0356(6)
P18	1	0.3608(2)	0.62061(19)	0.32737(7)	0.0385(6)
P19	0.856(3)	0.09669(16)	0.35536(16)	0.32880(6)	0.0468(5)
Sb19	0.144(3)	0.09669(16)	0.35536(16)	0.32880(6)	0.0468(5)
P20	0.704(3)	0.09699(12)	0.15695(13)	0.17698(5)	0.0479(4)
Sb20	0.296(3)	0.09699(12)	0.15695(13)	0.17698(5)	0.0479(4)
P21	1	0.44604(17)	0.68156(17)	0.20069(7)	0.0280(5)

All atoms lie on Wyckoff sites 4*g*. Note that U_{eq} is defined as one third of the trace of the orthogonalized U_{ij} tensor.

Table S3: Anisotropic displacement parameters[a] [Å^2] of $P_{20.56(1)}Sb_{0.44(1)}$, space group *P*2/*c*.

Atom	U_{11}	U_{22}	U_{33}	U_{12}	U_{13}	U_{23}
P1	0.0209(7)	0.0238(8)	0.0245(8)	−0.0035(6)	0.0024(6)	0.0030(6)
P2	0.0180(7)	0.0222(8)	0.0363(9)	−0.0023(6)	0.0074(6)	0.0036(6)
P3	0.0188(7)	0.0276(8)	0.0277(9)	0.0048(6)	0.0070(6)	−0.0081(6)
P4	0.0171(7)	0.0216(7)	0.0256(8)	−0.0031(6)	0.0078(6)	0.0013(6)
P5	0.0203(8)	0.0255(8)	0.0264(8)	0.0041(6)	0.0017(6)	−0.0057(6)
P6	0.0182(7)	0.0223(7)	0.0341(9)	0.0037(6)	0.0041(6)	−0.0096(6)
P7	0.0205(7)	0.0261(8)	0.0279(9)	0.0056(6)	0.0042(6)	−0.0059(6)
P8	0.0184(7)	0.0206(7)	0.0281(9)	0.0022(6)	0.0086(6)	−0.0012(6)
P9	0.0171(7)	0.0225(8)	0.0248(8)	−0.0040(6)	0.0048(6)	0.0020(6)
P10	0.0192(7)	0.0226(7)	0.0267(8)	−0.0056(7)	0.0061(6)	0.0027(6)
P11	0.0186(7)	0.0258(8)	0.0240(8)	0.0025(6)	0.0076(6)	−0.0044(6)
P12	0.0166(7)	0.0198(7)	0.0209(8)	−0.0033(6)	0.0085(6)	−0.0005(6)
P13	0.0189(7)	0.0225(8)	0.0275(8)	−0.0019(6)	0.0064(6)	0.0040(6)
P14	0.0173(7)	0.0229(7)	0.0280(8)	0.0033(6)	0.0054(6)	−0.0047(6)
P15	0.0177(7)	0.0244(8)	0.0244(8)	0.0001(6)	0.0053(6)	−0.0029(6)
P16	0.0164(7)	0.0216(7)	0.0208(8)	0.0062(6)	0.0066(6)	0.0005(6)
P17	0.0404(9)	0.0459(10)	0.0196(8)	0.0138(8)	0.0068(7)	0.0007(7)
P18	0.0488(10)	0.0460(10)	0.0143(8)	0.0222(9)	−0.0021(7)	−0.0046(7)
P19	0.0540(9)	0.0513(9)	0.0305(8)	0.0061(7)	0.0039(6)	0.0037(6)
Sb19	0.0540(9)	0.0513(9)	0.0305(8)	0.0061(7)	0.0039(6)	0.0037(6)
P20	0.0425(6)	0.0542(7)	0.0449(7)	−0.0049(5)	0.0084(4)	−0.0079(5)
Sb20	0.0425(6)	0.0542(7)	0.0449(7)	−0.0049(5)	0.0084(4)	−0.0079(5)
P21	0.0287(7)	0.0341(9)	0.0209(7)	−0.0018(7)	0.0067(6)	0.0005(6)

[a]The anisotropic displacement factor exponent takes the form: $-2\pi^2[(ha^*)^2U_{11}+\ldots+2hka^*b^*U_{12}]$.

Table S4: Interatomic distances [Å] in $P_{20.56(1)}Sb_{0.44(1)}$. All distances within d_{max} = 2.6 Å are listed. Standard deviations are smaller than 0.3 pm.

P1:	P8	2.199	P12:	P11	2.199
	P2	2.209		P13	2.202
	P17	2.228		P4	2.281
P2:	P1	2.209	P13:	P12	2.202
	P3	2.217		P14	2.207
	P10	2.272		P19|Sb19	2.290
P3:	P4	2.204	P14:	P15	2.198
	P2	2.217		P13	2.207
	P18	2.226		P6	2.288
P4:	P3	2.204	P15:	P16	2.197
	P5	2.278		P14	2.198
	P12	2.281		P20|Sb20	2.393
P5:	P6	2.205	P16:	P15	2.197
	P4	2.208		P9	2.198
	P19|Sb19	2.326		P8	2.278
P6:	P5	2.205	P17:	P21	2.154
	P7	2.215		P9	2.226
	P14	2.288		P1	2.228
P7:	P6	2.215	P18:	P21	2.127
	P8	2.218		P11	2.219
	P20|Sb20	2.397		P3	2.226
P8:	P1	2.199	P19|Sb19:	P13	2.290
	P7	2.218		P5	2.326
	P16	2.278		P20|Sb20	2.529
P9:	P16	2.198	P20|Sb20:	P15	2.393
	P10	2.217		P7	2.397
	P17	2.226		P19|Sb1	2.529
P10:	P11	2.209	P21:	P18	2.127
	P9	2.217		P17	2.154
	P2	2.272		P21	2.177
P11:	P12	2.199			
	P10	2.209			
	P18	2.219			

References:

1. Liu, X. K.; Ang, K. W.; Yu, W. J.; He, J. Z.; Feng, X. W.; Liu, Q.; Jiang, H.; Tang, D.; Wen, J.; Lu, Y. M.; Liu, W. J.; Cao, P. J.; Han, S.; Wu, J.; Liu, W. J.; Wang, X.; Zhu, D. L.; He, Z. B., Black Phosphorus Based Field Effect Transistors with Simultaneously Achieved Near Ideal Subthreshold Swing and High Hole Mobility at Room Temperature. *Sci. Rep.-Uk* **2016**, *6*, 24920.
2. Li, L. K.; Yu, Y. J.; Ye, G. J.; Ge, Q. Q.; Ou, X. D.; Wu, H.; Feng, D. L.; Chen, X. H.; Zhang, Y. B., Black Phosphorus Field-Effect Transistors. *Nat. Nanotechnol.* **2014**, *9*, 372-377.
3. Liu, B. L.; Kopf, M.; Abbas, A. N.; Wang, X. M.; Guo, Q. S.; Jia, Y. C.; Xia, F. N.; Weihrich, R.; Bachhuber, F.; Pielnhofer, F.; Wang, H.; Dhall, R.; Cronin, S. B.; Ge, M. Y.; Fang, X.; Nilges, T.; Zhou, C. W., Black Arsenic-Phosphorus: Layered Anisotropic Infrared Semiconductors with Highly Tunable Compositions and Properties. *Adv. Mater.* **2015**, *27*, 4423-4429.
4. Schusteritsch, G.; Uhrin, M.; Pickard, C. J., Single-Layered Hittorf's Phosphorus: A Wide-Bandgap High Mobility 2D Material. *Nano Lett.* **2016**, *16*, 2975-2980.